Annals of R.S.C.B., ISSN:1583-6258, Vol. 25, Issue 3, 2021, Pages. 6836 - 6845
Received 16 February 2021; Accepted 08 March 2021.

X-ray Analysis by Williamson-Hall Methods of Pure and Doped ZnO Nanoparticles

Ashwaq T. Alani[1], Tagreed M. Al- Saadi[2*]
[1'2]College of Education for Pure Science/Ibn Al- Haitham, University of Baghdad, Baghdad, Iraq
Email: taghreed.m.m@ihcoedu.uobaghdad.edu.iq

Abstract: $Zn_{0.8}Cr_XNi_{0.2-X}$ (where X=0, 0.05, 0.1, 0.15, 0.2) nanopowders, by the citrate path, were synthesized by the auto-combustion sol-gel method and heat-treated at 700 ◦C. X-ray diffraction (XRD) analysis and electron microscopy with high-resolution scanning microscopy (SEM) have characterized the samples collected. In addition, an X-ray energy dispersive (EDX) study was carried out. Using Scherrer's formula and the Williamson-Hall (W-H) analysis, the average crystallite size and lattice strain were analyzed, assuming the (Uniform Deformation Model) (UDM), (Uniform Deformation Stress Model), (UDSM) and (The Energy Density Model for Uniform Deformation) (UDEDM). The results reveled that there was a strong association between the average of crystallite size and the lattice strain calculated from the different studies.

Keywords: Doped ZnO, Williamson-Hall, X-ray Analysis, Nanotechnology, Size –Strain Plot

1. INTRODUCTION

(ZnO) Zinc oxide is recognized as a significant semiconductor that has been studied importantly in the last decades. Because of its technological and fundamental importance. ZnO has a high excitation binding energy of about (~60 meV) and a wide bandgap about (~3.37 eV) [1, 2]. Crystal morphology and particle size at room temperature play essential roles in many applications, which have made many researchers concentrate on the synthesis of the nanostructure of zinc oxide. Hence, many methods to synthesize the ZnO consist of precipitation [3], solo-chemical processes [4], DC thermal plasma synthesis [5], combustion synthesis [6], pyrolysis [7], spray pyrolysis [8], physical vapor deposition, micro-emulsion method [9], hydrothermal synthesis [10, 11] and a sol-gel method [12] and co-precipitation [13]. Among all pervious methods, the sol-gel method is convenient for synthesizing ZnO nanoparticles because of its flexibility, so an easy and cost-effective technique was performed in the present study.

In all directions to infinity, a perfect crystal will extend, thus because of their finite size, no crystals are perfect. This difference in perfect crystallinity leads to an expansion of the peaks of diffraction. The two primary properties that were derived from the analysis of peak width is (a) crystallite size and (b) lattice strain. Crystallite size is a measure of the coherence of the size from the peak of diffraction [14]. Owing to the presence of polycrystalline aggregates [15], the crystallite size of the particles is not necessarily the same as the particle size. Transmission electron microscopy (TEM) and Scanning electron microscopy (SEM) analysis are the most common techniques used for the calculation of particle size rather than crystallite size.

Annals of R.S.C.B., ISSN:1583-6258, Vol. 25, Issue 3, 2021, Pages. 6836 - 6845
Received 16 February 2021; Accepted 08 March 2021.

Owing to the forming of polycrystalline aggregates, the crystallite size of the particles is not exactly the similarly as the size of particle. The lattice dislocations can cause the lattice strain, but there are other strain causes, like the triple junction of the boundaries of the grain, contact or sinter stresses, accumulate faults, and stresses of coherence, etc. The measurement of diffraction peak broadness enables the determination of two significant features: the size of the crystallite and, the strain of the lattice. A size measure of coherently diffracting domains is the crystallite size, and the lattice strain is a measure of the distribution of the lattice constants resulting from disorders of crystals [16].

For the investigation of dislocation distribution, X-ray line broadening is used. Mechanical alloying causes a considerable amount of pressure in the powders, in addition to crystallite size reduction and alloying [17].

The pseudo-Voigt functions, Rietveld refinement, and Warren-Averbach analysis [18] are among the available methods to estimate the crystallite size and lattice pressure. A simplified integral breadth approach is the analysis of Williamson-Hall (W-H) in which both size-induced and strain-induced expansion are de convoluted by considering the peak broadness as a function of 2 θ [19].

This study, represents a comparative estimate of the average particle size of $Zn_{0.8}Cr_XNi_{0.2-X}$ (where X=0, 0.05, 0.1, 0.15, 0.2) nanoparticles obtained from direct SEM measure and peak expansion of powder X-ray diffraction. The strain correlating with the prepared $Zn_{0.8}Cr_XNi_{0.2-X}$ samples after annealed at 700 °C because of lattice deformation by a modified form of W-H, namely the uniform deformation model (UDM). As a function of 'U' energy density, the other modified models, such as the Uniform Deformation Stress Model (UDSM) and the Uniform Deformation Energy Density Model (UDEDM), gave an idea of the relationship between stress-strain and strain. In UDM, the isotropic form of the crystal is considered, while UDSM and UDEDM assume that the crystal is anisotropic [16].

In the present study, the strain linked to the hexagonal crystal's anisotropic existence is contrasted. Then drawn with the strain resulting from the interplanar spacing. It reported such surveys on $Zn_{0.8}Cr_XNi_{0.2-X}$ (where X=0, 0.05, 0.1, 0.15, 0.2) nanoparticles synthesized laconically and qualitatively by the sol-gel process. For estimating crystallite size and lattice strain, W-H analysis is used. Although X-ray profile analysis is an average method, apart from SEM micrographs, they still hold an unavoidable position for grain size determination.

2. EXPERIMENTAL DETAILS

$Zn_{0.8}Cr_XNi_{0.2-X}$ were prepared by auto combustion technique. All precursors that used were chromium nitrate $Cr(NO_3)3.9H2O$, zinc nitrate $Zn(NO_3)_2.6H_2O$, nickel nitrate $Ni(NO_3)_2.6H_2O$, Citric acid $C_6H_8O_4$, ammonia solution (NH_3), and distilled water. To prepare 10 grams of pure zinc oxide nanoparticles, distilled water was mixed with (Ni, Zn, Cr) nitrate and (7.07196 g) of citric acid as its percentage was constant for each sample. The materials were mixed for 40 min, by a magnetic stirrer at room temperature and it started raising the temperature of the solution until it stabilized at 100 ℃ and the water has begun to evaporate, and became a dry gelatinous liquid and begins to ignite. By using ceramic mortar to get rid of lumps, and get the nanopowder.

Annals of R.S.C.B., ISSN:1583-6258, Vol. 25, Issue 3, 2021, Pages. 6836 - 6845
Received 16 February 2021; Accepted 08 March 2021.

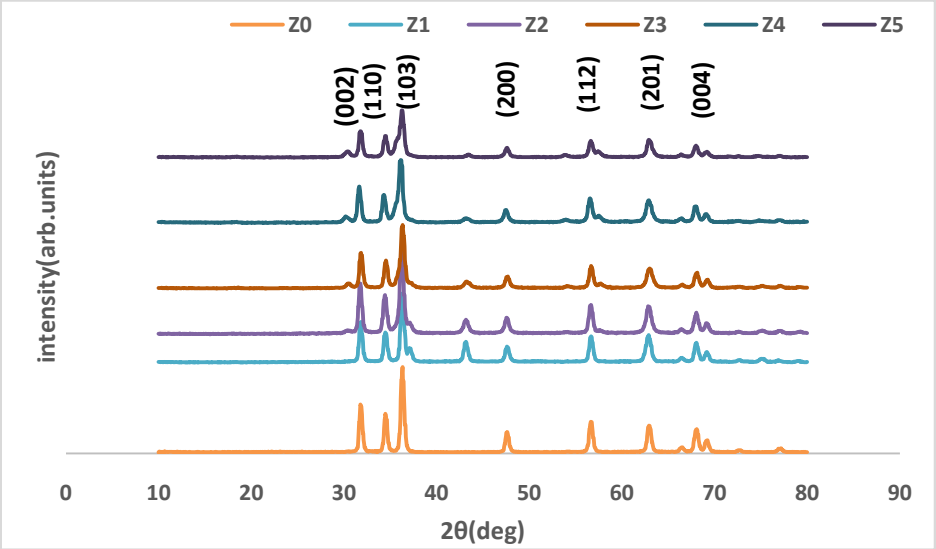

A sole-gel combustion technique was used in this study to prepare- $Zn_{0.8}Cr_XNi_{0.2-X}$ NPs. The compound was prepared (where X=0, 0.05, 0.1, 0.15, 0.2). It is used with the comparative studies particle size of Zn 0.8CrXNi0.2-X -NPs from the powdered XRD are dealt with.

3. RESULTS AND DISCUSSION

3.1.X-ray Diffraction

The purity of the phase and crystal construction of the synthesized ZnO and Zn 0.8CrXNi0.2-X -NPs annealed at 700°C, were investigated by using X-ray diffraction. The standard XRD spectra shown in Figure (1) are $Cr_xNi_{0.2-x}O$ pure ZnO and Zn0.8 for the value of (x) as the Cr material with nano-particles (x= 0, 0.05, 0.10, 0.15, and 0.20). The patterns of XRD have shown that the diffraction peaks return to pure ZnO nanoparticles. It can be indexed to a structure of hexagonal wurtzite. Four clear peaks of zinc oxide can be detected from the patterns, within range of (10o-80o), assigned to the planes of (1 0 1), (1 0 0), (0 0 2), (0 0 2), and (1 10). The dominant orientation was (101) on the surface, which corresponds well to the regular ZnO of (JCPDS 36-1451, (a=b=0.3279 nm), and (c= 0.5204 nm)), with a space group of (P63mc). The structure (wurtzite) is proposed to be unchanged, for all different doping concentrations. A small change was observed for doped samples in the peaks of the diffraction pattern relative to the un-doped ZnO sample. From Table 1 it can notice that the presence of chromium and nickel ions, which have ionic radii of 75.5 pm and 83 pm respectively, has led to the small size of the unit cell due to the process of their substitution for the zinc ion of ionic radius 88 pm. The survival of the zinc phase was unchanged, indicating that the ion exchange process occurred. The unit cell parameters were calculated by using “fullprof” software and the results are shown in Table.1.

Annals of R.S.C.B., ISSN:1583-6258, Vol. 25, Issue 3, 2021, Pages. 6836 - 6845
Received 16 February 2021; Accepted 08 March 2021.

Fig. 1. X- Ray pattern of the $Zn_{0.8}Cr_xNi_{0.2-x}$ (x= 0 , 0.05, 0.10, 0.15, and 0.20) samples.

Table.1.Unit cell parameters of pure ZnO nanoparticles and doped with Cr, Ni

Sample	Unit Call parameters		Call Volume ($Å^3$)
	a (Å)	C (Å)	
ZnO	3.249	5.203	47.57
$Zn_{0.8}Ni_{0.2}O$	3.248	5.202	47.54
$Zn_{0.8}Cr_{0.05}Ni_{0.15}O$	3.246	5.198	47.42
$Zn_{0.8}Cr_{0.1}Ni_{0.1}O$	3.248	5.201	47.52
$Zn_{0.8}Cr_{0.15}Ni_{0.05}O$	3.242	5.193	46.75
$Zn_{0.8}Cr_{0.2}O$	3.249	5.203	47.56

3.2. Crystallite Size and Strain

3.2.1. Scherrer Method

Due to dislocation, XRD can be used to analyze peak enlargement with crystallite size and lattice strain [20]. The crystallite size of the ZnO nanoparticles was specified by the X-ray line extension technique using the Scherer equation.

$$D = \frac{K\lambda}{\beta_{hkl}\cos\theta} \quad \text{---------- (1)}$$

Where K indicates to the Scherrer's constant (the shape factor) = 0.9, λ = 1.5406 Å is the wavelength of the event CuKα radiation; β represents the full-width at half maximum and θ is the Bragg diffraction angle. A mixture of both instrument- and sample-dependent effects is the width of the Bragg peak. In order to disunite these contributions, to determine the breadth, it is important to gather a diffraction pattern from the line widening of standard material. The instrument-corrected β-expansion corresponding to the ZnO diffraction peak was calculated utilizing the next equation [21].

$$\beta^2_{hkl} = \beta^2_{measur\ ed} + \beta^2_{instrumental} \quad \text{---------- (2)}$$

3.2.2. Williamson–Hall (W-H) Method

3.2.2.1. The Uniform Deformation Model (UDM)

The Williamson-Hall analysis is a simplified approach of integral breadth, differentiating the peak of the deformation caused by pressure consider the expanding width of the peak as a function of the diffraction angle and particle size. In compliance with these Williamson-Hall methods. The individual contribution of the line enlargement of a Bragg can be expressed as: [22]

$$\beta^2_{hkl} = \beta^2_D + \beta^2_\varepsilon \text{---------- (3)}$$

$$\beta_{hkl}\cos\theta = \frac{k\lambda}{D} + 4\varepsilon\sin\theta \text{---------- (4)}$$

Where (D) is the average of the particle size of an X-ray diffraction peak, the (βε) and (β_D) particle size and the contribution of the particle size are Strain to peak extension, (βhkl) at half-maximum peak (radiant) is the full width and (ε) is the micro strain. Inside, Eq. 2 The strain in

Annals of R.S.C.B., ISSN:1583-6258, Vol. 25, Issue 3, 2021, Pages. 6836 - 6845
Received 16 February 2021; Accepted 08 March 2021.

all crystal directions was assumed to be uniform, suggesting a uniform model of deformation. The word (sinθ) is plotted versus (β_{hkl} cosθ) and illustrates the consequence of uniform deformation analysis. The success from the slope of the fitted line, the particle size can be calculated to reflect the strain [23].

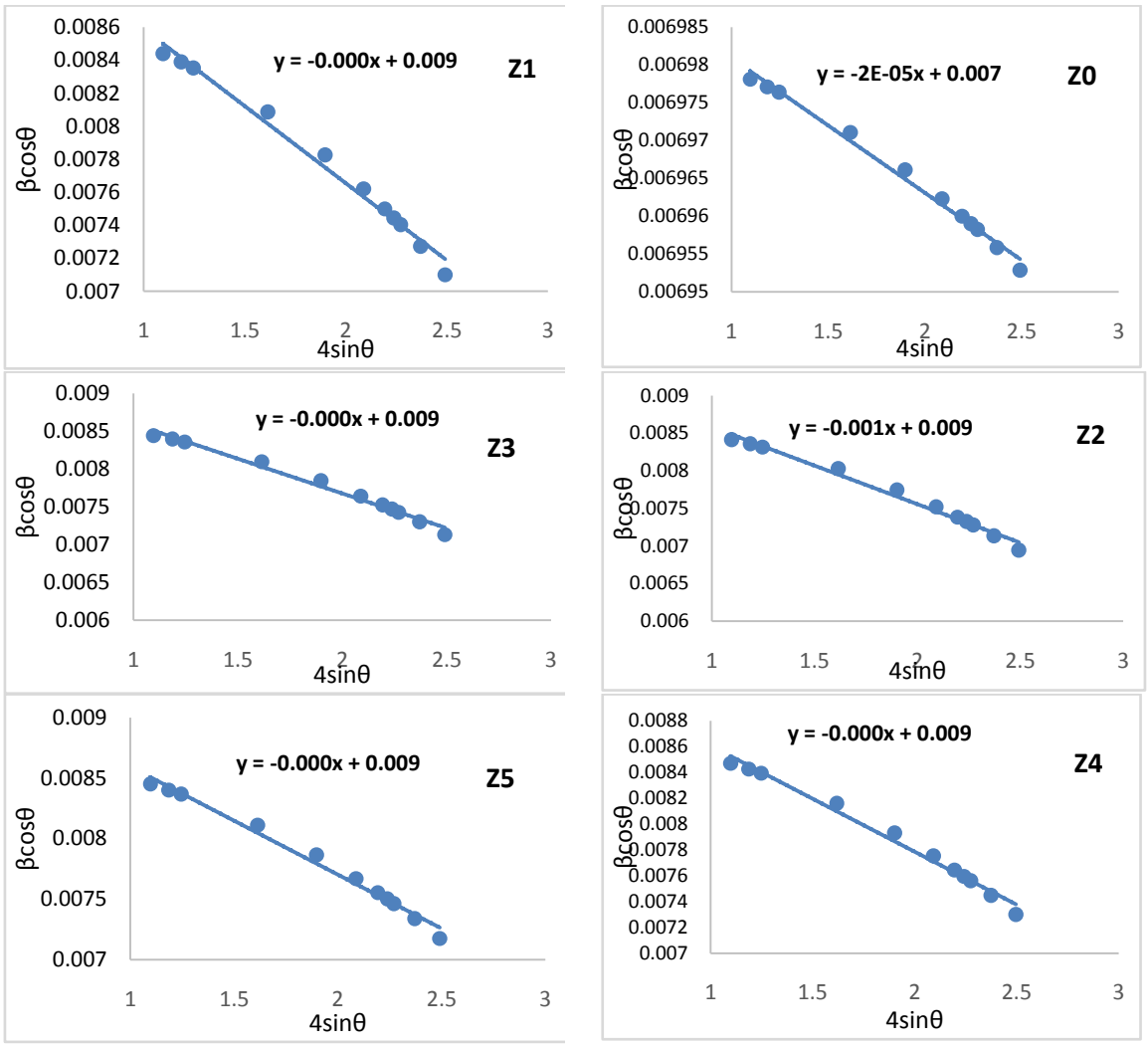

Fig. 2. Plot of β_{hkl} cosθ vs 4sinθ of $Zn_{0.8}Cr_xNi_{0.2-x}$ (x= 0, 0.05, 0.10, 0.15, and 0.20) nanoparticles.

3.2.2.2. Uniform stress deformation model (USDM)

Linear proportion relationship between strain (ε) and stress there was a beyond the elastic limit, depending on the Hooke's law, ($\sigma = Y\varepsilon$) there was σ(where Y: is called the Young modulus or modulus of elasticity. Furthermore ,Affair approximation of the noticeably small strain is this formula. Consequently, the lattice deformation stress is assumed to be uniform in the second term of the equation. The UDM sense and to the band is to be using this Eq. replaced ε=σ/Y while the updated Eq. (4) was the display as below:

$$\beta_{hkl} cos\theta = \frac{k\lambda}{D} + \frac{4\sigma sin\theta}{Y_{hkl}} \text{ ---------- (5)}$$

Annals of R.S.C.B., ISSN:1583-6258, Vol. 25, Issue 3, 2021, Pages. 6836 - 6845
Received 16 February 2021; Accepted 08 March 2021.

Here, Y_{hkl} is the Young module in the usual direction of the (hkl) planes set. The straight-line slope between β_{hkl} cosθ and 4sinθ/Y_{hkl} shows the stress [24, 25]. The modulus of Young is related to its elastic compliances for all samples with the phase of a hexagonal crystal for ZnO S_{11}= 7.858 x10^{-12}, S_{13} 2.206 x10^{-12}, S_{33}=6.94x10^{-12}, S_{44}= 23.57 x10^{-12} m ^{2}N $^{-1}$[26]

$$Y_{hkl} = \frac{[h^2 + \frac{(h+2k)^2}{3} + \frac{(al)^2}{c}]^2}{S_{11}\left[h^2 + \frac{(h+2k)^2}{3}\right]^2 + S_{33}(\frac{al}{c})^4 + (2S_{13} + S_{44})[h^2 + \frac{(h+2k)^2}{3}](\frac{al}{c})^2} - - - (6)$$

Where the elastic compatibilities of ZnO are S11, S13, S33, S44.

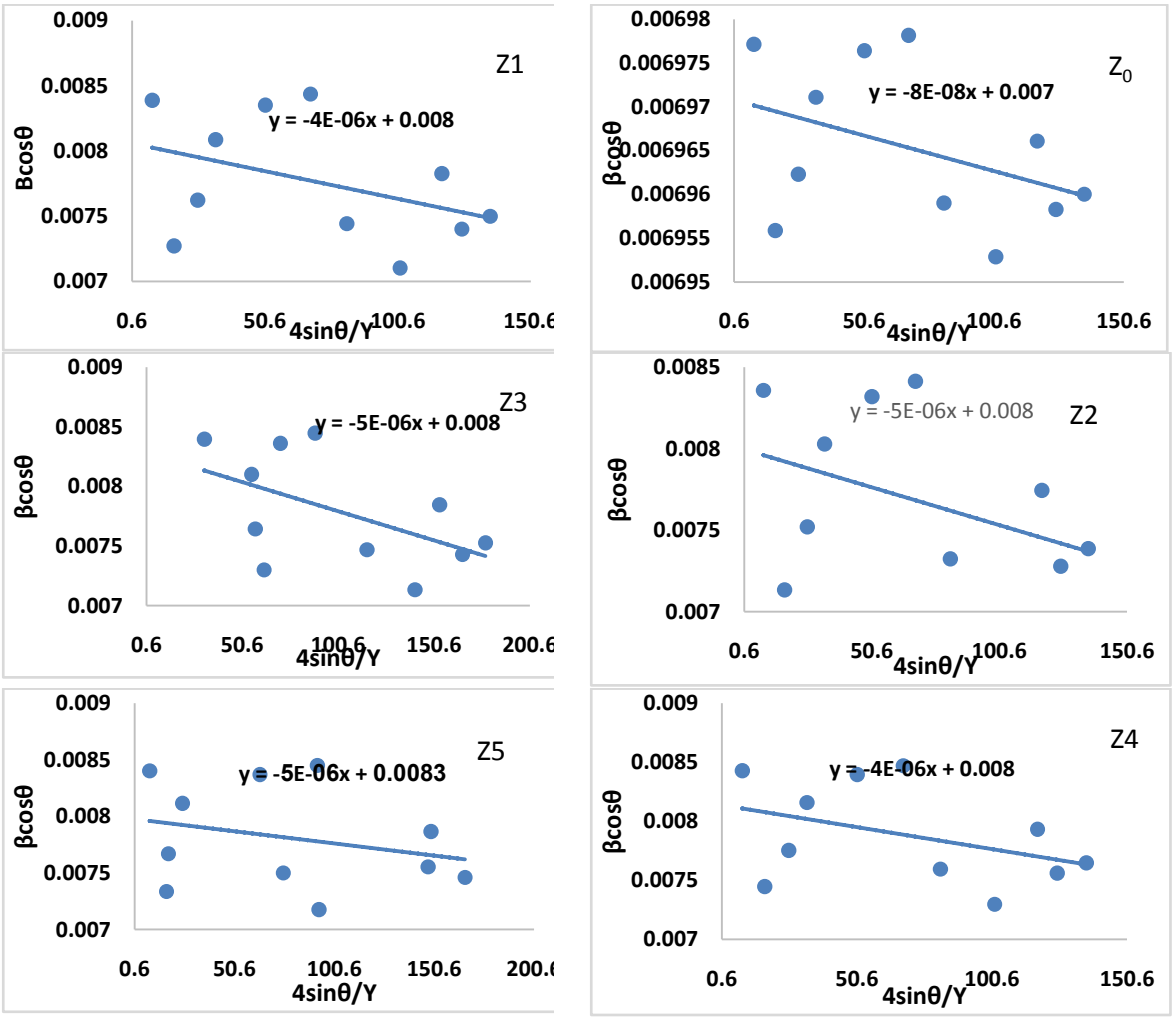

Fig. 3. The modified Williamson-Hall analysis of $Zn_{0.8}Cr_xNi_{0.2-x}$ (x= 0, 0.05, 0.10, 0.15, and 0.20) nanoparticles assuming USDM.

3.2.2.3. Uniform deformation energy density model (UDEDM)

The stress, particle size, strain parameters, can be found using this Uniform Deformation Energy Density Model and Density of Energy. It is assumed that the crystals earlier in the equation have isotropic and homogeneous crystals (4). It is not justified in multiple situations. In addition, this proportion

Annals of R.S.C.B., ISSN:1583-6258, Vol. 25, Issue 3, 2021, Pages. 6836 - 6845
Received 16 February 2021; Accepted 08 March 2021.

correlated with the strain-stress ratio is not when the energy density (u) is assumed to be broadly independent, moreover, when considering the energy density (U), this proportion linked to the strain-stress ratio is not extensively independent. The energy density (U) the following equation can be determined from the U=□^{2}Y$_{hkl}$/2 relation (5) can therefore be modified to fit the strain and energy relationship by utilizing the subsequent equation [27, 28].

$$\beta_{hkl}\cos\theta = \frac{k\lambda}{D} + (4sin\theta(\frac{2U}{Y_{hkl}})^{\frac{1}{2}}) \quad ---------- (7)$$

And 4sinθ (2/Y$_{hkl}$)$^{1/2}$ from the line slope plotted between $\beta_{hkl}\cos\theta$

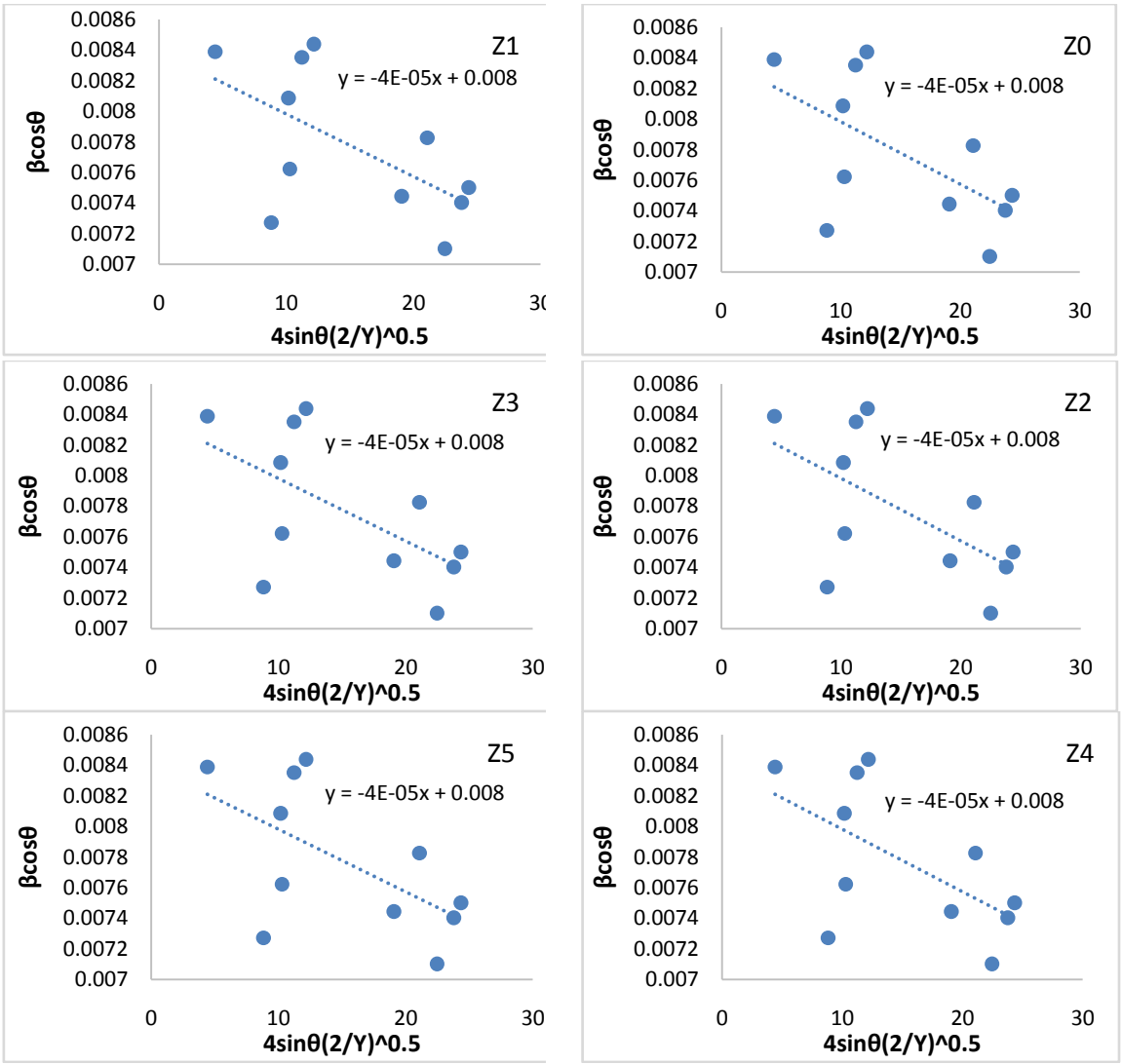

Fig. 4. The modified Williamson - Hall analysis of $Zn_{0.8}Cr_xNi_{0.2-x}$ (x= 0, 0.05, 0.10, 0.15, and 0.20) nanoparticles assuming UDEDM.

Annals of R.S.C.B., ISSN:1583-6258, Vol. 25, Issue 3, 2021, Pages. 6836 - 6845
Received 16 February 2021; Accepted 08 March 2021.

Table 2. Lattice strain, crystallite size, and deformation stress determined from diverse models.

	UDM			**USDM**			**UDEDM**			
Sample	Scherrer D Å	W-H D Å	Micro Strain $\times10^{-3}$	W-H D Å	Micro Strain $\times10^{-5}$	σ Pa $\times10^{-6}$	W-H D Å	Micro Strain $\times10^{-4}$	σ $\times10^{-5}$	U 10^{-10} Jm
Z_0	199.6	198.1	-0.02	198.1	-0.155	-0.08	198.1	0.0499	0.0256	0.0064
Z_1	179.12	146	-0.9	171.2	-7.79	-4	165.1	2.49	1.28	16
Z_2	181.36	144.4	-1	173.3	-9.74	-5	165.1	2.49	1.28	16
Z_3	178.65	146	-0.9	167.1	-22.1	-5	157.6	4.71	1.06	25
Z_4	176.38	147.5	-0.8	171.2	-7.79	-4	165.1	2.49	1.28	16
Z_5	178.07	146	-0.9	167.1	-9.10	-5	165.1	1.81	0.994	9

3.2. SEM and EDX

SEM testing proved that the prepared powders were within the nanoscale at an approximate rate of 31.3 nm. On the other hand, its shapes were spherical and semi-spherical, and some of them were hexagonal.

EDX testing proved the existence of all the elements involved in preparing the examined sample, and the peaks appeared at the energies Kα = 8.637 keV, Kα = 0.525 keV, Kα = 5.415 keV, and, Kα = 7.480 keV which belong to the elements according to the sequence Zinc, Oxygen, Chromium, and Nickel as seen in Fig.6.

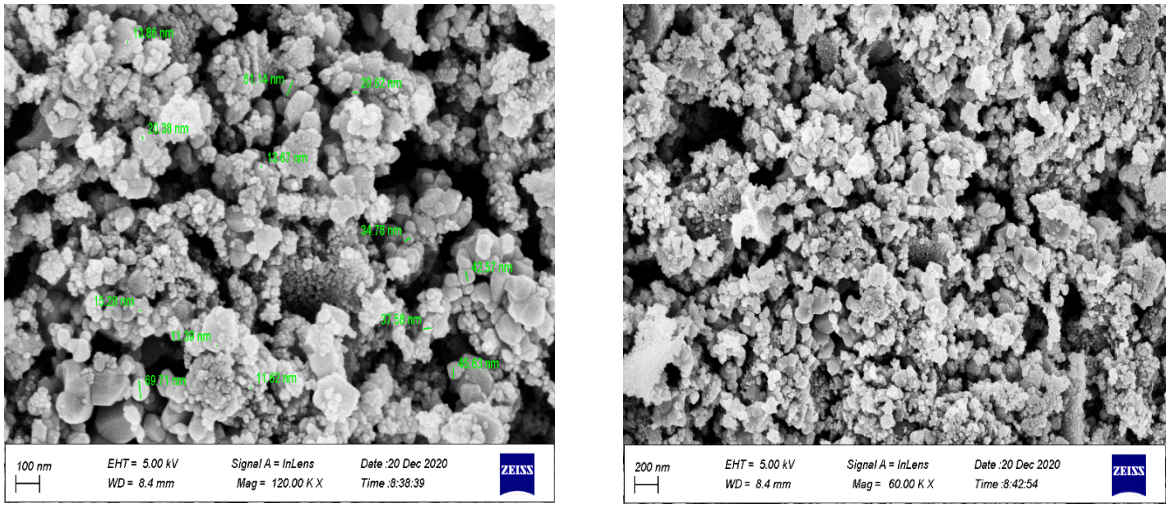

Fig. 5. SEM image of the sample Z4

Annals of R.S.C.B., ISSN:1583-6258, Vol. 25, Issue 3, 2021, Pages. 6836 - 6845
Received 16 February 2021; Accepted 08 March 2021.

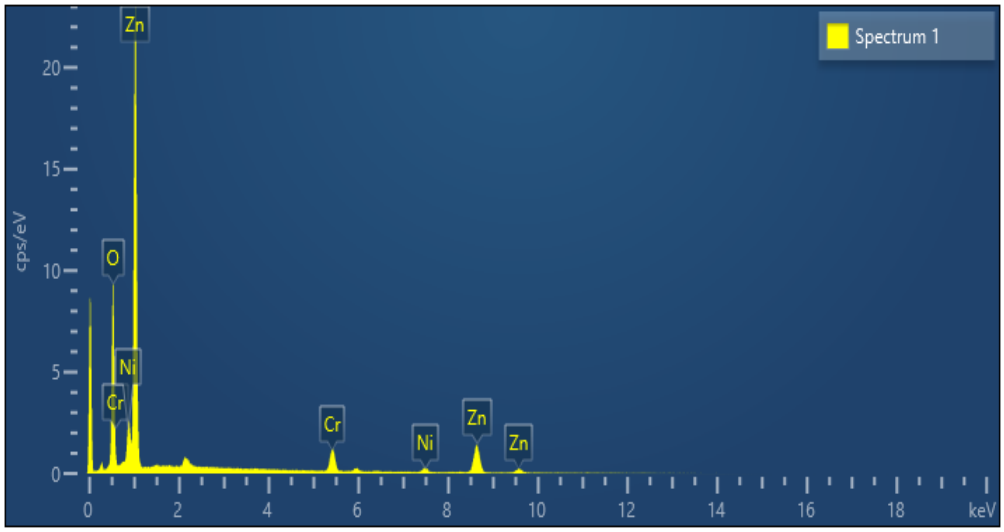

Fig. 6. EDX graph of the sample Z4

4. CONCLUSION

ZnO nanocrystals were synthesized using the Sol-Gel technique. For nano zinc oxide characterization, Techniques for SEM and powder XRD are used. The broadening of the peak line is due to internal stress and crystal size, based on the X-ray diffraction patterns of zinc oxide nanoparticles. Using Scherrer's formula and the Williamson-Hall equation, these parameters were investigated. The improved version of the W-H model is sufficient for the investigation of the Size of the crystal and strain those results from distortion of the lattice.

The strain of lattice ε is not the same as that described by UDSM and UDEDM, if an anisotropic crystalline with a cubic nature is assumed. Moreover, the image of a scanning electron microscope (D = 31.3nm) confirmed the nano-crystalline state of the annealed ZnO.

Centered on UDM, UDSM and UDEDM, the Williamson-Hall system Models are useful for the accurate measurement of the values of crystal size, strain, stress and energy density. Therefore, to grasp the crystal refinement, these models are very sensible. The estimated crystal size value based on the Williamson-Hall method is consistent with that calculated from SEM images (average crystal size 31.3 nm).

REFERENCES

1. Y.Masuda, N. Kinoshita,F.Sato, K. Koumoto, ACS, *Design* 2006, **6**, 1, 75–78.
2. N.S. Minimala, A. John Peter, J. Nano- Electron. Phys. 4 No 4, 04004 (2012).
3. A. Amiable, M.T. Buscaglia, V. Buscaglia, P. Bowen, J. Eur. Ceram. Soc. **30** (2010), 591-598.
4. M.R. Vaezi, S.K. Sadrnezhaad, Mater. Des. **28**, 515-519
5. T.S. Ko, S. Yang, H.C. Hsu, C.P. Chu, H.F. Lin, S.C. Liao, T.C. Lu, H.C. Kuo, W.F. Hsieh,S.C.Wang Mater.Sci, and Eng. B.**134**(2006)54.
6. N. Riahi-Noori, R. Sarraf-Mamoory, P. Alizadeh, A. Mehdikhani, J.Ceram. Process. Res. **9** (2008)246.

7. W.S. Chiu, P.S. Khiew, D. Isa, M. Cloke, S. Radiman, R. Abd-Shukor, M.H. Abdullah, N.M. Huang, Chem. Eng. J. **142** (2008) 337.
8. S.B. Park, Y.C. Kang, J. Aerosol. Sci. **28** (1997) 473.
9. T.V.Kolekar, H.M.Yadav, S.S.Bandgar, A.C.Raskar, S.G.Rawal and G.M.Mishra, I. S. R J. V. -1, Feb (2011).
10. W. Bai, K. Yu, Q. Zhang, X. Zhu, D. Peng, Z. Zhu, N. Dai, Y. Sun, Physica E Low Dimens. Syst. Nanostruct. **40**, 822(2008).
11. H. Bai,X. Liu, Mater. Mater Lett. **64**, 341-343(2010).
12. J. Ungula, M.Sc. thesis, Dep.Ph, U. F. S. (QwaQwa campus), South Africa, (2015).
13. V. D. Mote, V. R. Huse, B. N. Dole, WJCMP , **2**, 208-211, (2012).
14. Vd Mote, Y Purushotham, and Bn Dole,J. Theor. Appl. Phys., **6**, (1) 2012. Doi: 10.1186/2251-7235-6-6.
15. Ramakanth, K: Basics of X-ray Diffraction and its Application. I.K. International Publishing House Pvt. Ltd., New Delhi (2007).
16. S. Devesa, A.P. Rooney, M.P. Graça, D. Cooper, L.C. Costa" Mater. Sci. Eng". 263 (2021).
17. Cullity, BD, Stock, SR: Elements of X-ray diffraction, 3rd ed. Prentice Hall Publication, India (2001).
18. Balzar, D, Ledbetter, H: J. Appl. Crystallogr. **26**, 97 (1993).
19. 19 Suryanarayana, C, Grant Norton, M: X-ray Diffraction: A Practical Approach. Springer, New York (1998)
20. R. Yogamalar, R. Srinivasan, A. Vinu, K. Ariga, A.C. Bose, Solid State Commun. **149**, 1919 (2009).
21. Y.T. Prabhu, K. V. Rao, V. S. Sai Kumar, B.S. Kumari , WJNSE, **4** (1) 21-28, (2014).
22. Biju V, Sugathan N, Vrinda V, Salini SL, J. Mater. Sci, **l** (43) 1175–1179, (2008).
23. M.S. Geetha, H. Nagabhushana, H.N. Shivananjaiah, J. Sci. Adv. Mat. Devices, **1** 301-310, (2016).
24. H. Irfan, M. Racik K, and S. Anand, J. Asian Ceram. Soc. **6**(1) 54- 62, 2018.
25. T. M. K. Thandavan, S. M. A. Gani, C. San Wong, and R. M. Nor, J. Nondestruct. Eval. **34**, (2) 14, 2015.
26. Nye, JF: Physical Properties of Crystals: Their Representation by Tensors and Matrices. Oxford, New York (1985).
27. Ahmed H. Abed, Ziad T. Khodair, Tagreed M. Al-Saadi, and Tariq A. Al-Dhahir, AIP Conference Proceedings **2123**, 020019 (2019); https://doi.org/10.1063/1.5116946.
28. H. Irfan, Mohamed Racik K. and S. Anand, J. Asian Ceram. Soc. **6**(1) 54–62, (2018).